NANO LETTERS

pubs.acs.org/NanoLett

Large Enhancement of Nonlinear Optical Phenomena by Plasmonic Nanocavity Gratings

Patrice Genevet,[†,§] Jean-Philippe Tetienne,[†] Evangelos Gatzogiannis,[‡] Romain Blanchard,[†] Mikhail A. Kats,[†] Marlan O. Scully,[§,∥] and Federico Capasso*[,†,§]

[†]School of Engineering and Applied Sciences and [‡]Center for Nanoscale Systems, Harvard University, Cambridge, Massachusetts 02138, United States, [§]Institute for Quantum Studies and Department of Physics, Texas T&M University, College Station, Texas 77843, United States, and [∥]College of Engineering and Applied Science, Princeton University, Princeton, New Jersey 08544, United States

ABSTRACT Enhancing nonlinear processes at the nanoscale is a crucial step toward the development of nanophotonics and new spectroscopy techniques. Here we demonstrate a novel plasmonic structure, called plasmonic nanocavity grating, which is shown to dramatically enhance surface nonlinear optical processes. It consists of resonant cavities that are periodically arranged to combine local and grating resonances. The four-wave mixing signal generated in our gold nanocavity grating is enhanced by a factor up to ≈2000, 2 orders of magnitude higher than that previously reported.

KEYWORDS Surface plasmons, localized plasmons, plasmonic nanocavity, grating, nonlinear optics

Plasmonics is concerned with the manipulation of light at the nanoscale. It involves the study of the coupling between electromagnetic radiation and collective electronic oscillations in metals, known as surface plasmons.[1,2] The resulting field enhancement makes them particularly attractive for surface nonlinear optics, since the efficiency of most nonlinear phenomena can be greatly enhanced.[3−10] Potential applications include nanophotonics and spectroscopy where nonlinear optical processes play an important role, either for frequency conversion or to detect chemical fingerprints.

While isolated metal particles have been extensively studied,[5] patterned substrates have received much less attention. Recently, Renger et al. showed that four-wave mixing (4WM) in a gold substrate can be enhanced by patterning the surface with a grating and exploiting evanescent waves.[10] Gratings have also been used to enhance the 4WM process by phase matching the generated signal with the pump beam.[11] Here we report on a novel approach based on plasmonic nanocavity gratings to enhance surface nonlinear processes. We have designed plasmonic nanocavities, made of nanogrooves in a gold film,[12,13] and arranged them periodically to combine local resonances of the nanocavities with grating resonances that involve surface plasmon polaritons (SPPs) propagating on the corrugated surface. Since the corrugation is composed of resonant structures, the properties of SPPs along such an interface are considerably affected. To avoid any confusion with SPPs propagating at a flat metal−dielectric interface, we generally refer to these modes as surface waves.

Several works already proposed to interpret such an interaction between localized and delocalized plasmons in the context of Fano resonances.[14−16] We apply this concept of coupled resonances to 4WM in gold and demonstrate an enhancement of the generated signal of up to ≈2000 compared with an unpatterned surface, 2 orders of magnitude higher than that reported in ref 10. This result shows that plasmonic nanocavity gratings are a promising route to enhancing optical nonlinearities in the metal and also in any material filling the cavities, with potential applications to nanoscale frequency conversion and highly sensitive vibrational spectroscopy and microscopy.

A single narrow groove (tens of nanometers wide) defined on a metal surface can be viewed as a portion of a metal−insulator−metal (MIM) waveguide terminated by a metallic mirror on one side and a dielectric mirror (air) on the other. It therefore forms a cavity that sustains Fabry−Pérot modes.[13] Because the cavity mode is confined in a subwavelength volume, large fields are established both in the metal and in the dielectric under resonant excitation.[13] In addition to these localized surface plasmons (LSPs), a grating of nanogrooves enables the coupling of free space light to surface waves (SWs) propagating on the corrugated surface. Figure 1 illustrates schemes to couple light into (a) or out of (b) a nanocavity via excitation of SWs. Because they combine both LSPs and SWs and can exhibit a very high density of electromagnetic energy, nanogroove gratings are an ideal tool for enhancing various nonlinear optical phenomena. In our experiment, two laser beams, E_1 at frequency ω_1 and

* To whom correspondence should be addressed.
Received for review: 08/4/2010
Published on Web: 11/03/2010

DOI: 10.1021/nl102747v | *Nano Lett.* **2010,** *10,* 4880–4883

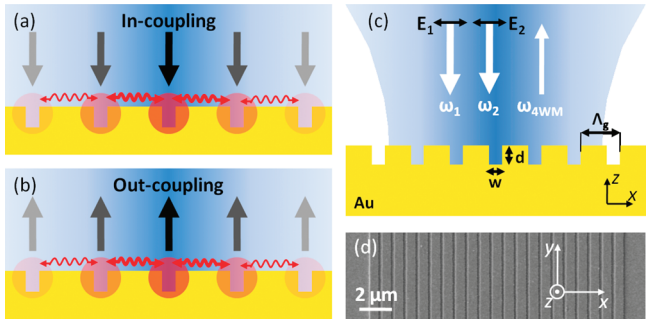

FIGURE 1. Nanogroove gratings in a metal surface can enhance nonlinear phenomena due to high field enhancement involving both localized and propagating surface plasmons. (a) Light is coupled into a localized nanocavity mode, assisted by propagating surface plasmons (red wavy arrows). (b) An emitter positioned in a groove exhibits enhanced emission and collimation effect. (c) Schematic of the four-wave mixing experiment. Two normally incident beams at ω_1 and ω_2 are focused on the corrugated gold structure and generate light at the four-wave mixing frequency $2\omega_1 - \omega_2$, enhanced by the nanocavity grating. (d) SEM image of a typical nanogroove grating ($w = 100$ nm, $d = 90$ nm, $\Lambda_G = 600$ nm).

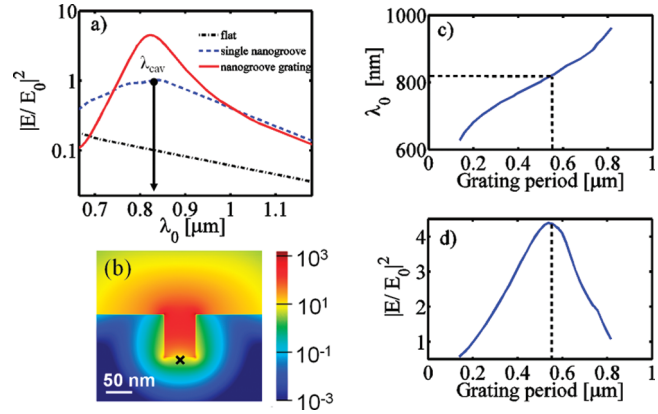

FIGURE 2. (a) Field intensity beneath a single groove (blue dashed line), beneath a groove grating with period $\Lambda_G = 560$ nm (red line), and beneath a flat surface (dashed black line). E_0 is the incident wave field. The field is evaluated inside the metal 5 nm away from the interface, as indicated by the black X in (b). The grooves are 60 nm wide and 90 nm deep, and light is a normally incident Gaussian beam with a 1 μm waist. The arrow indicates the nanocavity resonance (λ_{cav}). (b) Field distribution $|E/E_0|^2$ at resonance ($\lambda_0 = 820$ nm for $\Lambda_G = 560$ nm) in the vicinity of a groove in the grating. (c) Resonance wavelength of the nanogroove grating vs Λ_G. (d) Field intensity at resonance vs Λ_G divided by the incident intensity. The dashed line correspond to the "double resonance" condition (i.e., $\lambda_0 = n_g\lambda_g = n_g\Lambda_G = \lambda_{cav}$, coincidence of grating and nanogroove resonance). As the grating period is changed, the electromagnetic field enhancement decreases because the resonance condition with the nanocavity is lost (i.e., $\lambda_0 = n_g\lambda_g = n_g\Lambda_G \neq \lambda_{cav}$).

E_2 at ω_2, are focused onto the structure with both beams polarized perpendicularly to the groove direction (Figure 1c). A scanning electron microscope (SEM) image of a typical fabricated grating is shown in Figure 1d.

To elucidate the optical properties of nanogroove gratings, we performed numerical simulations using the finite difference time domain (FDTD) method. Details are provided in Supporting Information. Figure 2a shows the electric field intensity as a function of the excitation wavelength, monitored in the metal within the skin depth, 5 nm below the bottom of an isolated groove (dashed blue line), 60 nm wide and 90 nm deep. For reference, we show the field intensity in the case of a flat surface (dot-dashed black line). All fields are normalized to that of the incident wave ($|E_0|$). We observe the fundamental cavity resonance at $\lambda_0 = \lambda_{cav,1} =$ 820 nm. As depicted in Figure 1a, a nanogroove grating offers additional paths, relying on SWs, to couple free space photons into LSPs. Assuming an infinite grating with period Λ_G illuminated by a plane wave with free space wavevector $k_0 = 2\pi/\lambda_0$, momentum conservation for coupling photons to SWs propagating at the corrugated interface requires $k_0 \sin(\alpha) + q\beta_G = k_g$ where α is the angle of incidence, q an integer, $\beta_G = 2\pi/\Lambda_G$, and $k_g = 2\pi/\lambda_g = n_g k_0$ is the SW wavevector, λ_g and n_g being the effective wavelength and mode index, respectively, of the SW propagating along the nanogroove grating surface. However, this condition is relaxed because of the distribution of incident angles for a focused beam. Parts c and d of Figure 2 show the dependence of the coupled wavelength $\lambda_0 = n_g\lambda_g$ and the field intensity, respectively, on Λ_G. Note that the coupled wavelength is controlled by the grating period ($\lambda_0 = n_g\lambda_g = n_g\Lambda_G$ where n_g strongly depends on the frequency), and that the energy stored in the nanogrooves is maximum when $\lambda_0 = \lambda_{cav,1}$. In summary, the highest electric fields in the grooves are obtained when the grating launches SWs corresponding to an incident wavelength which is also resonant with the intrinsic cavity mode ($\lambda_0 = n_g\lambda_g = n_g\Lambda_G = \lambda_{cav,1}$). For 60 nm wide 90 nm deep grooves, the grating period which satisfies this condition is $\Lambda_G \approx 560$ nm. The corresponding spectrum, which is asymmetric, is shown in Figure 2a (red curve), and a color map of the electric field intensity at the resonance wavelength $\lambda_0 = 820$ nm is shown in Figure 2b. We see in Figure 2b that the electric field is maximum, in the metal, near the groove bottom ($|E/E_0|^2 \sim 10$), and in the air, near the groove entrance ($|E/E_0|^2 \sim 10^3$). This suggests that the structure could be used to enhance nonlinear optical processes not only in the dielectric filling the grooves but also in the metal. A local enhancement factor for the electric field in the metal can be defined as $\eta_{in} = |E/E_{flat}|$ where E_{flat} refers to the electric field beneath a flat metal surface, E and E_{flat} are calculated at the same depth below the metal−dielectric interface. The subscript *in* denotes the in-coupling process (Figure 1a).

In the following, we consider the nonlinear mixing of two near-infrared beams at $\lambda_1 = 820$ nm and $\lambda_2 = 1064$ nm, respectively. The third-order nonlinear response of gold, characterized by its susceptibility tensor $\chi^{(3)}$ (on the order of 8×10^{-19} (m/V)^2 [17]), gives rise to fields oscillating at frequencies $2\omega_1 - \omega_2$ and $2\omega_2 - \omega_1$. For experimental convenience, we consider only the frequency up-conversion $\omega_{4WM} = 2\omega_1 - \omega_2$, resulting in light generation at $\lambda_{4WM} = 667$ nm. The nonlinear polarization can then be expressed as $P^{(3)}(\omega_{4WM}) = \chi^{(3)}E_1{}^2E_2{}^*$. We define the local enhancement factor of the 4WM process as

DOI: 10.1021/nl102747v | *Nano Lett.* **2010,** *10,* 4880–4883

$$(\mathrm{EF})_{\mathrm{I}} = \eta_{\mathrm{in},1}^4 \eta_{\mathrm{in},2}^2 \eta_{\mathrm{out,4WM}}^2 \quad (1)$$

where $\eta_{\mathrm{in},i}$ is the local field enhancement at ω_i, $\eta_{\mathrm{out,4WM}}^2 = P_{\mathrm{rad}}/P_{\mathrm{rad,flat}}$, and P_{rad} is the power radiated by an infinitesimal volume of polarized medium in the metal ($P_{\mathrm{rad,flat}}$ refers to a flat surface, see details in the Supporting Information). Thus, η_{out} enables us to quantify the out-coupling from the above volume, taking into account the local field enhancement as well as the collimation effect of the grating, the optical losses, and the collection efficiency (Figure 1b).

Since $(\mathrm{EF})_{\mathrm{I}}$ varies as the fourth power of $\eta_{\mathrm{in},1}$, we expect that the largest 4WM intensity is obtained by optimizing the in-coupling process at the frequency ω_1. We therefore fixed the depth $d = 90$ nm to achieve localized resonance at λ_1 and varied w and Λ_{G}.

We fabricated nanogroove gratings with widths w ranging from 60 to 240 nm and periods Λ_{G} ranging from 200 to 800 nm. Each fabricated grating is 13 μm by 13 μm in size, much larger than the beam waist (≈1 μm for our 40× objective). The fabrication process involved electron-beam lithography on a silicon substrate, evaporation of gold followed by lift-off, which defines w and d, followed by another E-beam deposition of gold.

The experimental apparatus is based on a typical coherent anti-Stokes Raman scattering (CARS) microscopy setup.[20] It employs mode-locked lasers to generate the incident synchronous picosecond pulses at λ_1 and λ_2. Schematic and details are provided in the Supporting Information.

The experimental results are presented in Figure 3a, where we study the dependence of the 4WM enhancement as a function of w and Λ_{G}. We obtained the latter by normalizing the measured 4WM signal to the one measured from a flat surface (see Supporting Information for a discussion on the relation between this overall enhancement and the local one $(\mathrm{EF})_{\mathrm{I}}$, eq 1). For a given period, the 4WM signal increases as w decreases due to the larger field enhancement for narrower grooves.[13] On the other hand, three maxima appear when Λ_{G} is varied, namely, at $\Lambda_{\mathrm{G}} \approx 300$ nm, $\Lambda_{\mathrm{G}} \approx 560$ nm, and $\Lambda_{\mathrm{G}} \approx 720$ nm. They can be understood by considering the dependence of $\eta_{\mathrm{in},1}^4$, $\eta_{\mathrm{in},2}^2$, and $\eta_{\mathrm{out,4WM}}^2$ on Λ_{G} (panels b–d of Figure 3). Indeed, each η_i is maximized when Λ_{G} satisfies the coupling condition to the SWs at normal incidence ($\Lambda_{\mathrm{G}} = \lambda_{\mathrm{g},i}$). The maximum 4WM enhancement (≈2000) is obtained when $\eta_{\mathrm{in},1}^4$ is maximized, as expected given the dependence of $(\mathrm{EF})_{\mathrm{I}}$ on $\eta_{\mathrm{in},1}^4$ in eq 1. While the widths of the peaks in Figure 3b,c, and d are related to the distribution of angles for a focused beam, the combined effect of the enhancement factor of each frequency has to be considered to explain the features appearing in Figure 3a. We note that the measured overall enhancement around $\Lambda_{\mathrm{G}} \approx 560$ nm does not decay as rapidly as expected from the calculations as the groove width is increased. This effect

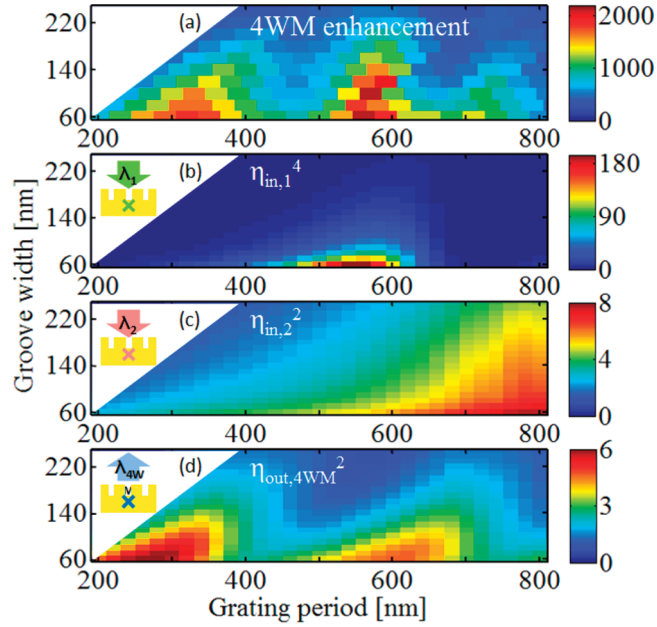

FIGURE 3. (a) Measured 4WM signal as a function of the groove width w and the grating period Λ_{G}. The experimental data are normalized to the 4WM signal obtained from an unpatterned gold surface and show a maximum enhancement of ≈2000. (b, c) Simulated enhancement factor $\eta_{\mathrm{in},1}^4$ (b) and $\eta_{\mathrm{in},2}^2$ (c), evaluated 5 nm below the groove bottom (see inset). (d) Simulated enhancement factor $\eta_{\mathrm{out,4WM}}^2$, evaluated by monitoring the power radiated by a small volume of polarized medium (see inset and Supporting Information). Both $\eta_{\mathrm{in},1}$ and $\eta_{\mathrm{in},2}$ exhibit a maximum when $\Lambda_{\mathrm{G}} = \lambda_{\mathrm{g},i}$, which explains the variation of the 4WM enhancement with Λ_{G} in (a). In (d), a higher order surface waves coupling condition also appears for $\Lambda_{\mathrm{G}} = 2\lambda_{\mathrm{g,4WM}}$.

can most likely be attributed to surface roughness or local imperfections that create uncontrolled field enhancement.

In addition to wave mixing, noble metals exhibit nonlinear absorption in the near-infrared and visible ranges. In particular, two-photon-excited luminescence (TPEL) is a well-known phenomenon that has been extensively studied.[18,19] In gold, this process gives rise to spectrally broad luminescence with a local maximum around $\lambda \approx 650$ nm.[18] In our experiment, TPEL is also considerably enhanced compared to an unpatterned gold surface.

Figure 4a shows the measured power at $\lambda = 667$ nm as a function of the power P_1 impinging on the sample at ω_1, with $P_2 = 32$ mW. We observe a transition from two-color ($\omega_1 + \omega_2$) TPEL to 4WM as P_1 is increased. This interpretation is justified by the linear dependence of the emitted signal on both P_1 (Figure 4a, slope = 1) and P_2. When P_1 exceeds about 10 mW (peak intensity ≈ 2.4 GW/cm^2), the dependence changes to quadratic while it remains linear for P_2 (inset in Figure 4a), as expected for 4WM. We note that a small background signal, much weaker than the 4WM signal, is observed when only E_1 is present ($E_2 = 0$) due to single frequency ($\omega_1 + \omega_1$) TPEL.

Finally, we studied the polarization dependence of the measured signal in the 4WM regime (Figure 4b). We first measured the polarization of the 4WM signal which was

DOI: 10.1021/nl102747v | *Nano Lett.* **2010,** *10,* 4880–4883

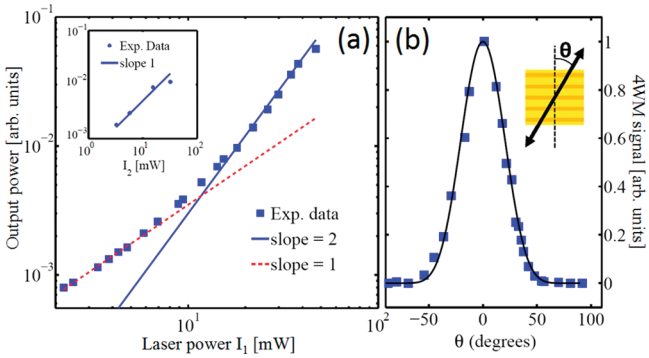

FIGURE 4. (a) Measured output power as a function of the incident power P_1 (log−log scale) for a typical nanogroove grating. Two regimes are observed. The dependence is linear for low laser power indicating that two-color TPEL is dominant. For higher laser power, about 10 mW, it becomes quadratic, indicating that 4WM dominates. Inset: Output power as a function P_2 for $P_1 = 20$ mW. (b) Output power when rotating the sample (all polarizations are kept fixed, see inset). Squares represent experimental data (a, b) while the curves are power laws in (a) and a $\cos^8(\theta)$ law in (b).

found to be normal to the grating. We then inserted a polarizer in both the input and output beam paths and measured the variation of the 4WM signal when the sample is rotated. Figure 4b shows that the measured 4WM signal follows a $\cos^8(\theta)$ law, where θ is the angle between the grating and the input and output polarizations (inset in Figure 4b). Physically, this dependence results from the fact that only those components of the electric field which are normal to the grating couple to the nanocavity grating modes and therefore are enhanced by the structure. Thus, each η_i varies as $|\cos(\theta)|$; hence the overall dependence on $\cos^8(\theta)$ (see eq 1).

In conclusion, we experimentally demonstrated an enhancement by more than 3 orders of magnitude of the third-order nonlinear response of gold by patterning the surface with a grating of resonant plasmonic nanocavities. We studied the influence of the grating period and explained the observed features as due to excitation of surface waves propagating at the corrugated interface, which strongly enhance coupling of light into and out of the grooves. In addition to 4WM and TPEL from the gold substrate, we expect that other nonlinear optical phenomena can be significantly enhanced by our structure. For example, the nanocavities can be filled with molecules or materials of interest, enabling potential applications to nanophotonic devices, nonlinear optics, and spectroscopy.

Acknowledgment. M.O.S. and P.G. acknowledge NSF Grant No. EEC-0540832 (MIRTHE ERC), the Office of Naval Research, and the Robert A. Welch Foundation (A-1261). The Harvard University work was supported by the NSF Nanoscale Science and Engineering Center (NSEC), the center for Nanoscale Systems (CNS) at Harvard University, a member of the National Nanotechnology Infrastructure Network (NNIN), and the Institute for Quantum studies at Texas A&M University. J.P.T. is supported by the École Normale Supérieure de Cachan, France. M.A.K. is supported by the NSF through a Graduate Research Fellowship.

Supporting Information Available. Details of the experimental setup, FDTD simulations (in-coupling and out-coupling), and the physical interpretation of the enhancement factor. This material is available free of charge via the Internet at http://pubs.acs.org.

REFERENCES AND NOTES

(1) Maier, S. A. *Plasmonics: Fundamentals and Applications*; Springer: New York, 2007.
(2) Gramotnev, D. K.; Bozhevolnyi, S. I. *Nat. Photonics* **2010**, *4*, 83.
(3) Bouhelier, A.; Beversluis, M.; Hartschuh, A.; Novotny, L. *Phys. Rev. Lett.* **2003**, *90*, 13903.
(4) Lippitz, M.; van Dijk, M. A.; Orrit, M. *Nano Lett.* **2005**, *5*, 799.
(5) Palomba, S.; Danckwerts, M.; Novotny, L. *J. Opt. A: Pure Appl. Opt.* **2009**, *11*, 114030.
(6) Danckwerts, M.; Novotny, L. *Phys. Rev. Lett.* **2007**, *98*, No. 026104.
(7) Rautian, S. G.; Safonov, V. P.; Chubakov, P. A.; Shalaev, V. M.; Shtokman, M. I. *JETP Lett.* **1988**, *47*, 243.
(8) Kim, S.; Jin, J.; Kim, Y. J.; Park, I. Y.; Kim, Y.; Kim, S. W. *Nature* **2008**, *453*, 757.
(9) Coutaz, J. L.; Neviere, M.; Pic, E.; Reinisch, R. *Phys. Rev. B* **1985**, *32*, 2227.
(10) Renger, J.; Quindant, R.; Van Hulst, N.; Novotny, L. *Phys. Rev. Lett.* **2010**, *104*, No. 046803.
(11) Giorgetti, E.; Lambkin, P.; Li, Q.; Palchetti, L.; Sottini, S.; Grando, D.; Blau, W. *J. Opt. Soc. Am. B* **1995**, *12*, 58.
(12) Coyle, S.; Netti, M. C.; Baumberg, J. J.; Ghanem, M. A.; Birkin, P. R.; Bartlett, P. N.; Whittaker, D. M. *Phys. Rev. Lett.* **2001**, *87*, 176801.
(13) Miyazaki, H. T.; Kurokawa, Y. *Appl. Phys. Lett.* **2006**, *89*, 211126.
(14) Christ, A.; Zentgraf, T.; Tikhodeev, S. G.; Gippius, N. A.; Kuhl, J.; Giessen, H. *Phys. Rev. B* **2006**, *74*, 155435.
(15) Miroshnichenko, A. E.; et al. *Rev. Mod. Phys.* **2010**, *82*, 2257.
(16) Lukyanchuk, B.; et al. *Nat. Mater.* **2010**, *9*, 707.
(17) Boyd, R. W. *Nonlinear optics*, 3rd ed.; Academic Press: Amsterdam and Boston, 2008.
(18) Imura, K.; Nagahara, T.; Okamoto, H. *Appl. Phys. Lett.* **2006**, *88*, No. 023104.
(19) Boyd, G. T.; Yu, Z. H.; Shen, Y. R. *Phys. Rev. B* **1986**, *33*, 7923.
(20) Evans, C. L.; Xie, X. S. *Annu. Rev. Anal. Chem* **2008**, *1*, 883.

DOI: 10.1021/nl102747v | *Nano Lett.* **2010,** *10,* 4880–4883